

STABILITY CHARACTERISTICS OF TIME INTEGRATION SCHEMES FOR FINITE ELEMENT SOLUTIONS OF CONDUCTION-TYPE PROBLEMS

G. COMINI AND M. MANZAN

Istituto di Fisica Tecnica e di Tecnologie Industriali, Università di Udine, Viale Ungheria 43, 33100 Udine, Italy

ABSTRACT

Stability characteristics of two-level, time-integration algorithms are investigated, with particular reference to explicit schemes. Conditions for stability are expressed on the basis of algebraic estimates of the eigenvalues associated with the amplification matrices of the algorithm. The use of automatic symbolic manipulators allows an extension of these estimates to higher order and multidimensional elements. Eigenvectors are also evaluated algebraically and the resulting fundamental mode shapes are related to the onset of instabilities.

KEY WORDS Stability analysis Finite elements

INTRODUCTION

In the finite element solution of transient problems of the conduction-type, the so-called partial discretization technique is the most common approach. According to this procedure, the governing equations are first discretized in the space dimensions using, for example, the Galerkin method. Afterwards, the resulting sets of ordinary differential equations are integrated in time by means of suitable time-stepping schemes^{1,2}.

The schemes for time-integration must be accurate and simple but, to produce meaningful results, they must also be stable, at least conditionally. Implicit schemes, usually, are accurate and unconditionally stable but can be somewhat complex in programming and are generally very demanding with computer time. For this reason explicit schemes are often considered a viable alternative that avoids most difficulties, even if at the expense of conditional stability^{1–4}.

In this paper we investigate the stability characteristics of time-integration algorithms, with particular reference to explicit schemes. The main objective of this research is finding algebraic estimates of the maximum allowable time steps that can be used with explicit procedures of time integration. Only two-level schemes are considered since, in practical applications, they are usually preferred to multilevel schemes. In fact two-level schemes lead to single-step recurrence relations that have a very general applicability, allow easy adaptive variations of the time step and are always self-starting^{1,2}.

Conditions for stability are expressed on the basis of algebraic estimates of the eigenvalues associated with systems of space-discretized differential equations. The procedure is not a new one and, indeed, some classic results obtained by following this line of investigation are reported in most textbooks on the finite element method. However, published results concern almost invariably simple, one-dimensional elements, while it appears that little of a precise nature has been done for higher order and for two- and three-dimensional elements⁵. In this research

instead, the use of automatic symbolic manipulators has allowed us to extend considerably the range of algebraic estimates and, consequently, the applicability of matrix methods to the stability analysis of time-integration algorithms^{6,7}.

Once the eigenvalues have been found, a further point of great interest is the computation of the eigenvectors. The eigenvectors are associated to the fundamental mode shapes in which the solution vector responds to the forcing load. The numerical errors excite these modes and the resulting oscillations have a shape that is a combination of the fundamental modes^{8,9}.

STABILITY CHARACTERISTICS OF TWO-LEVEL TIME-INTEGRATION SCHEMES

The space discretization of many heat transfer and fluid flow problems of the conduction-type leads to sets of ordinary differential equations of the form:

$$\mathbf{C} \frac{\partial \phi}{\partial t} + \mathbf{K} \phi = \mathbf{f} \quad (1)$$

where t is the time, ϕ is the unknown vector, \mathbf{C} is the capacity matrix, \mathbf{K} is the conductance matrix and \mathbf{f} is the heat load vector^{1,2}.

Clearly, the stability characteristics of time-integration algorithms depend on the behaviour of the transient and, consequently, we are interested in the homogeneous form of (1)⁵. Thus, to perform a stability analysis, we can set $\mathbf{f} = 0$ and write the recurrence formula for time integration of (1) as:

$$\phi^{n+1} = \mathbf{A} \phi^n \quad (2)$$

where

$$\mathbf{A} = \left(\frac{1}{\Delta t} \mathbf{C} + \theta \mathbf{K} \right)^{-1} \left[\frac{1}{\Delta t} \mathbf{C} - (1 - \theta) \mathbf{K} \right] \quad (3)$$

is the amplification matrix, Δt is the time step and θ is a weighting factor.

The stability requirements of any time integration scheme are dependent on the eigenvalues of the amplification matrix \mathbf{A} , defined by the characteristic equation:

$$\mathbf{A} \phi_i = \mu_i \phi_i \quad (4)$$

where μ_i is the eigenvalue and ϕ_i is the corresponding eigenvector^{1,2}.

In stable schemes we must have:

$$|\mu_i| \leq 1 \quad (5)$$

for any eigenvalue μ_i of the matrix \mathbf{A} , since numerical errors must not be amplified from one step to the next. Condition (5) is always satisfied by implicit algorithms with $\theta > 1/2$ and, therefore, such algorithms are unconditionally stable. Instead, schemes with a weighting factor $\theta < 1/2$ satisfy (5) only for time steps that are smaller than a critical value and, therefore, such schemes are only conditionally stable. The critical value decreases with θ and the explicit algorithm, having $\theta = 0$, presents the smallest critical value of the time step. On the other hand, for $\theta = 0$, the time integration procedure becomes particularly simple and, if the matrix \mathbf{C} is replaced by its lumped equivalent \mathbf{C}_L , the solution is advanced in time without even the necessity of equation solving. Obviously, with explicit schemes, it is always convenient to use time steps that are as large as possible but remain within the limits for stability.

With two-level explicit schemes, putting $\theta = 0$ in (3), and substituting \mathbf{A} in (4) we obtain:

$$\Delta t \mathbf{C}^{-1} \left(\frac{1}{\Delta t} \mathbf{C} - \mathbf{K} \right) \phi_i = \mu_i \phi_i \quad (6)$$

Multiplying both sides of (6) by C and rearranging we have the generalized eigenproblem:

$$-K\phi_i = \frac{\lambda_i}{\Delta t} C\phi_i \tag{7}$$

in which the matrices K and C are positive definite and, consequently, the eigenvalues

$$\lambda_i = \mu_i - 1 \tag{8}$$

are real numbers greater or equal to zero^{1,10}.

Taking into account (8), we can express the stability condition (5) as:

$$|\lambda_i + 1| \leq 1 \tag{9}$$

which yields:

$$-2 \leq \lambda_i \leq 0 \tag{10}$$

The inequality $\lambda_i \leq 0$ at the right hand side is always satisfied while, to investigate the inequality $\lambda_i \geq -2$, it is sufficient to solve the characteristic equation

$$\det\left(-K - \frac{\lambda}{\Delta t} C\right) = 0 \tag{11}$$

with the global matrices replaced by the element matrices. In fact, it can be shown that the highest modulus of the global eigenvalues of (7) is always less than the highest modulus of the local element eigenvalues^{1,2,9}.

By referring to the characteristic equation (11), written for the element matrices, we obtain a number r of eigenvalues equal to the number of nodes in the element. Then, by considering the eigenvalues λ_i we can solve the eigenproblem (7) for $i = 1, r$ to obtain the r eigenvectors ϕ_i ¹⁰.

STABILITY CHARACTERISTICS OF FINITE ELEMENTS

In this research, the eigenvalues have been evaluated algebraically for several elements that are commonly employed in finite element analyses^{6,7}. Because of the current limitations of the algebraic manipulators, only the regular element shapes, represented in *Figures 1* and *2*, have been considered. The usual definitions have been assumed for the entries in the conductance matrix K :

$$K_{ij} = \int_{\Omega} \nabla N_i \cdot (k \nabla N_j) d\Omega = k \int_{\Omega} \nabla N_i \cdot \nabla N_j d\Omega \tag{12}$$

and for the entries in the consistent capacity matrix C :

$$C_{ij} = \int_{\Omega} N_i \rho c N_j d\Omega = \rho c \int_{\Omega} N_i N_j d\Omega \tag{13}$$

In the above equations, N_i and N_j are the shape functions, defined in terms of local coordinates, k is the thermal conductivity, ρc is the volumetric heat capacity and the domains Ω are defined in *Figures 1* and *2*. For linear elements we have considered also the lumped diagonal matrices C_L obtained from the consistent capacity matrices C by the row-summing technique:

$$(C_{ij})_L = \delta_{ij} \sum_k C_{ik} \tag{14}$$

where δ_{ij} is the Kronecker delta: $\delta_{ii} = 1$ and $\delta_{ij} = 0$ for $i \neq j$. For parabolic elements instead, lumped capacity matrices have not been computed, since for higher order elements there is no single agreed-upon method to diagonalise capacity matrices¹¹.

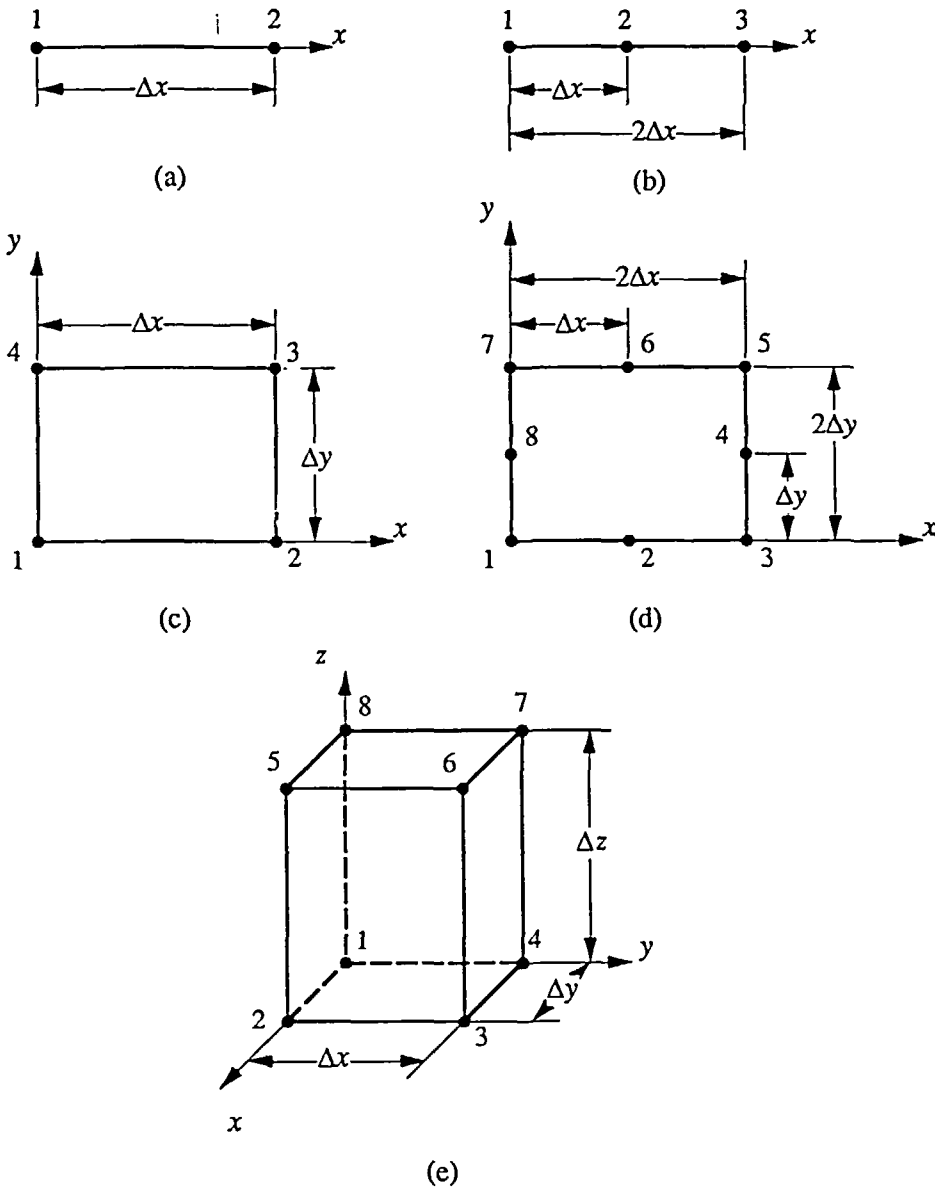


Figure 1 Characteristic dimensions of isoparametric elements: (a) one-dimensional linear elements; (b) one-dimensional parabolic elements; (c) two-dimensional linear elements; (d) two-dimensional parabolic elements; (e) three-dimensional linear elements

Matrices \mathbf{K} , \mathbf{C} and \mathbf{C}_L have been computed from equations (12) to (14). The results of these algebraic manipulations have been published elsewhere⁷ while, in Appendix A, we have listed the eigenvalues obtained automatically from the characteristic equation (11). In Appendix A, the eigenvalues are ordered according to their magnitude, at least whenever this criterion is applicable, and reference is always made to the diffusivity $\alpha = k/\rho c$ and to the dimensions defined in Figures 1 and 2.

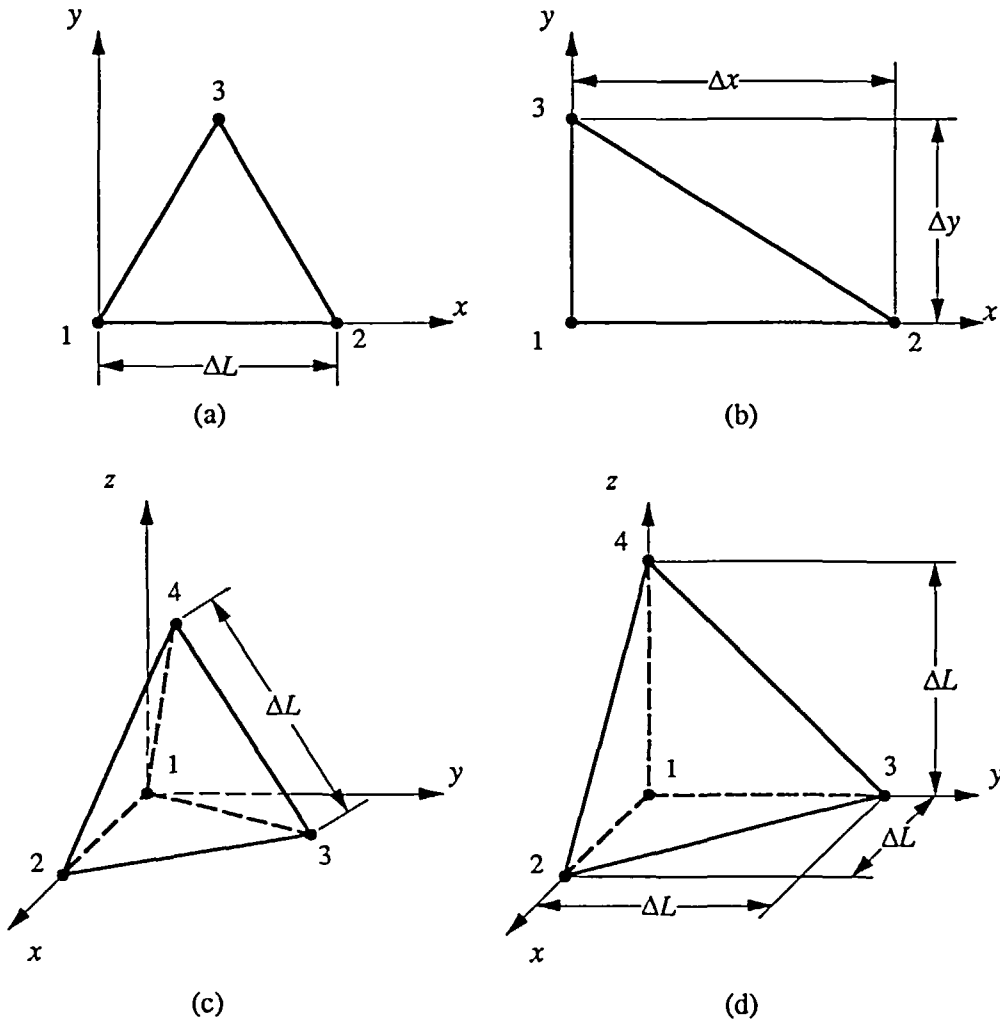


Figure 2 Characteristic dimensions of typical linear elements: (a) equilateral triangle; (b) right triangle; (c) equilateral tetrahedron; (d) rect tetrahedron

If we consider, for each element, the modulus of the largest eigenvalue, we can express the condition for stability, in dimensionless form, as:

$$Fo = \frac{\alpha \Delta t}{\Delta L^2} \leq -\frac{\lambda_M}{2} = Fo_{crit} = \frac{\alpha \Delta t_{crit}}{\Delta L^2} \tag{15}$$

where λ_M is the eigenvalue with the largest modulus, Fo is the Fourier number of the space-time discretization and the critical value Fo_{crit} is the maximum allowable dimensionless time step. The reference lengths ΔL and the values of Fo_{crit} are reported in Table 1 for all the elements analysed in Appendix A.

As we can see from Table 1, the stability analysis yields several results of practical interest. Consistent capacity matrices lead to more severe conditions for stability than lumped capacity matrices and the limitations on the time step increase also from one-dimensional to

Table 1 Characteristic dimensions ΔL and maximum allowable dimensionless time steps Fo for the one- (1D), two- (2D) and three- (3D) dimensional elements represented in Figures 1 and 2 referred to consistent (C) and lumped (L) capacity matrices

Element	ΔL	Fo_{crit}
1D—linear—C	Δx	1/6
1D—linear—L	Δx	1/2
1D—parabolic—C	Δx	2/15
2D—linear—C	$\left(\frac{1}{\Delta x^2} + \frac{1}{\Delta y^2}\right)^{-1/2}$	1/6
2D—linear—L	$\min(\Delta x, \Delta y)$	1/2
2D—parabolic—C	$\min\left[\left(\frac{1}{\Delta x^2} + \frac{5}{\Delta y^2}\right)^{-1/2}, \left(\frac{5}{\Delta x^2} + \frac{1}{\Delta y^2}\right)^{-1/2}\right]$	2/3
3D—linear—C	$\left(\frac{1}{\Delta x^2} + \frac{1}{\Delta y^2} + \frac{1}{\Delta z^2}\right)^{-1/2}$	1/6
3D—linear—L	$\min(\Delta x, \Delta y, \Delta z)$	1/2
equilateral triangle—C	ΔL	1/12
equilateral triangle—L	ΔL	1/3
right triangle—C	$\left(\frac{\Delta x^2 + \Delta y^2 + \sqrt{\Delta x^4 + \Delta y^4 - \Delta x^2 \cdot \Delta y^2}}{\Delta x^2 \cdot \Delta y^2}\right)^{-1/2}$	1/6
right triangle—L	$\left(\frac{\Delta x^2 + \Delta y^2 + \sqrt{\Delta x^4 + \Delta y^4 - \Delta x^2 \cdot \Delta y^2}}{\Delta x^2 \cdot \Delta y^2}\right)^{-1/2}$	2/3
equilateral tetrahedron—C	ΔL	1/20
equilateral tetrahedron—L	ΔL	1/4
rect tetrahedron—C	ΔL	1/40
rect tetrahedron—L	ΔL	1/8

multidimensional elements. In general, simpler or lower order elements perform better than higher order elements, at least as far as stability is concerned. However, rectangular elements show higher stability limits than right triangular elements having the same dimensions Δx and Δy . Similarly eight node, three-dimensional elements show higher stability limits than right tetrahedral elements having the same dimensions Δx , Δy and Δz .

The regularities in the eigenvalues are a further point of interest. All the elements have the first eigenvalue equal to zero. Besides, when isoparametric elements are compared, we can see that the eigenvalues of one-dimensional elements are a subset of the eigenvalues of two-dimensional elements, the eigenvalues of two-dimensional elements are a subset of the eigenvalues of three-dimensional elements and the eigenvalues of linear elements are a subset of the eigenvalues of parabolic elements.

Finally, it is worth noting that, whenever a non-uniform discretization is employed, the stability limit (15) is related to the smallest element in the mesh. However, with a non-uniform mesh, (15) might not hold good for small elements but might still be satisfied by large elements. In such cases oscillations arise in the small elements, where numerical errors are amplified, but these oscillations are filtered by the large elements, where numerical errors are reduced. Consequently, in a problem with a non-uniform mesh discretization, the stability condition (15) can be rather conservative, as demonstrated in Figure 3.

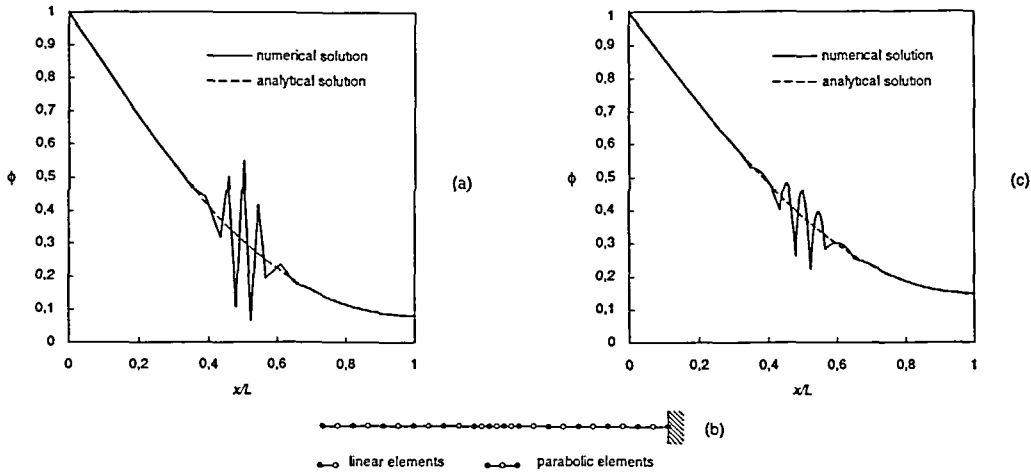


Figure 3 Onset of instabilities in one-dimensional heat conduction problems, with reference to the non uniform mesh discretizations represented in Figure 3b. (a) Solution at dimensionless time $at/L^2 = 0.1187$, obtained using linear elements and a time step $\Delta t = 145$ s smaller than the critical value $\Delta t'_{crit} = 480$ s for the large elements, but larger than the critical value $\Delta t''_{crit} = 120$ s for the small elements; (b) non-uniform discretizations using the same number of nodes but different number of linear and parabolic elements. (c) Solution at dimensionless time $at/L^2 = 0.1575$, obtained using parabolic elements and a time step $\Delta t = 125$ s smaller than the critical value $\Delta t'_{crit} = 400$ s for the large elements, but larger than the critical value $\Delta t''_{crit} = 100$ s for the small elements

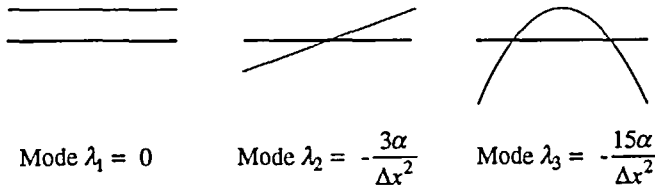


Figure 4 Eigenvalues of one-dimensional isoparametric elements. Models 1 and 2 are shared by linear and parabolic elements, while mode 3 is typical of parabolic elements

FUNDAMENTAL MODE SHAPES OF FINITE ELEMENTS

As we have already pointed out, the fundamental mode shapes in which the solution responds to the forcing load are related to the eigenvectors. The numerical errors excite these modes and the resulting numerical oscillations have a shape that is a combination of the fundamental modes. In particular, the largest eigenvalue is associated with the dominating eigenvector and the oscillations leading to numerical instabilities are likely to start with the shape corresponding to this dominating eigenvector.

In this research, the eigenvectors have been evaluated by solving automatically the eigenproblem (7) and the results obtained, for the elements represented in Figures 1 and 2, are reported in Appendix B. Obviously, the regularities in the eigenvalues are reflected into corresponding regularities of the eigenvectors. For example, we have always $\lambda_1 = 0$ and thus all the eigenproblems (7) have a corresponding first solution ϕ_1 that is a constant eigenvector. Besides, from Appendix B and Figures 4 and 5, we can see that the eigenvectors of three-dimensional isoparametric elements include the eigenvectors of two- and one-dimensional

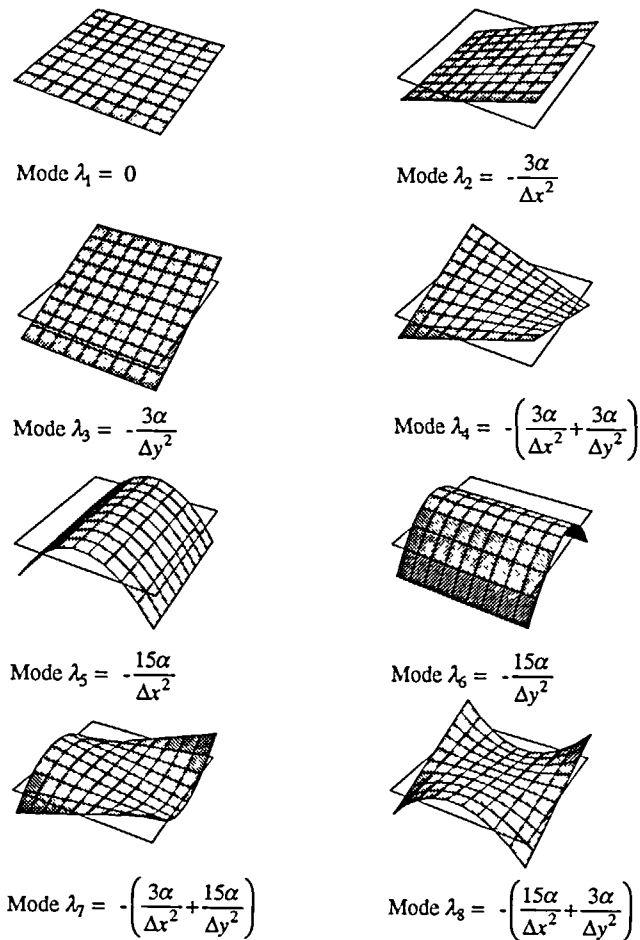


Figure 5 Eigenvectors of two-dimensional isoparametric elements. Modes 1 to 4 are shared by linear and parabolic elements, while modes 5 to 8 are typical of parabolic elements

isoparametric elements, while the eigenvectors of parabolic and two-dimensional isoparametric elements include, respectively, the eigenvectors of linear and one-dimensional isoparametric elements.

The graphical representations show clearly which eigenvector yields the dominating mode. The numerical experiments confirm that the dominating mode is the critical one for the onset of instabilities and, by looking at *Figures 3 and 4*, we can see that the shapes of the numerical oscillations correspond to the dominating eigenvectors. In fact, the dominating eigenvector is related to mode 2, i.e. to a '2 Δx ' wave pattern, for linear elements and to mode 3, i.e. to a parabolic wave pattern, for parabolic elements.

CONCLUSIONS

We have employed automatic symbolic manipulators to evaluate algebraically eigenvalues and eigenvectors of the generalized problem (7) with reference to several elements that are commonly used in finite element discretizations. This way, the range of applicability of matrix methods to stability analyses of time-integration algorithms has been greatly extended.

Because of the current limitations of the algebraic manipulators, only linear, time-independent problems and regular shapes of the elements have been considered. However, in the next future, the arrival of more powerful manipulators might remove these limitations and even open the way to analyses in which the global, instead of the element, amplification matrices might be considered.

REFERENCES

- 1 Zienkiewicz, O. C. and Morgan, K. *Finite Elements and Approximations*, Wiley, New York (1983)
- 2 Zienkiewicz, O. C. and Taylor, R. L. *The Finite Element Method*, Volume 2, 4th Edn, McGraw-Hill, London (1991)
- 3 Tacke, K. H. Discretization of the explicit enthalpy method for planar phase change, *Int. J. Num. Meth. Eng.*, **21**, 543–554 (1985)
- 4 Comini, G., Nonino, C. and Saro, O. Performance of enthalpy-based algorithms for isothermal phase change, in *Advanced Computational Methods in Heat Transfer* (Eds. L. C. Wrobel, C. A. Brebbia and A. J. Nowak), Vol. 3, pp. 3–13, Springer Verlag, Berlin (1990)
- 5 Hughes, T. R. J. *The Finite Element Method—Linear Static and Dynamic Finite Element Analysis*, Prentice Hall, London (1987)
- 6 Wolfram, S. *Mathematica—A System for Doing Mathematics by Computer*, 2nd Edn, Addison-Wesley, Redwood City, CA (1991)
- 7 Manzan, M. Algebraic solution of eigenproblems in stability analyses of finite-element algorithms for transient heat conduction (in Italian), *Quaderni Fis. Tecn.*, Università di Udine, 3 (1992)
- 8 Hirsch, C. *Numerical Computation of Internal and External Flows*, Volume 1, Wiley, New York (1988)
- 9 Irons, B. M. and Ahmad, S. *Techniques of Finite Elements*, Ellis Horwood, Chichester (1979)
- 10 Bathe, K. J. *Finite Element Procedures in Engineering Analysis*, Prentice-Hall, Englewood Cliffs, NJ (1982)
- 11 Zienkiewicz, O. C. and Taylor, R. L. *The Finite Element Method*, Volume 1, 4th Edn, McGraw-Hill, London (1989)

APPENDIX A

To save space, only the final expressions of eigenvalues are reported here, while the algebraic computations have been published elsewhere⁷. With reference to the elements represented in *Figures 1* and *2*, by going through the steps outlined in the text, we have obtained the following sets of eigenvalues:

— for one-dimensional, two-node linear elements, with consistent capacity matrices:

$$[\lambda_1, \lambda_2] = \left[0, -\frac{12\alpha}{\Delta x^2} \right] \quad (\text{A1})$$

— for one-dimensional, two-node linear elements, with lumped capacity matrices:

$$[\lambda_1, \lambda_2] = \left[0, -\frac{4\alpha}{\Delta x^2} \right] \quad (\text{A2})$$

— for one-dimensional, three-node parabolic elements, with consistent capacity matrices:

$$[\lambda_1, \dots, \lambda_3] = \left[0, -\frac{3\alpha}{\Delta x^2}, -\frac{15\alpha}{\Delta x^2} \right] \quad (\text{A3})$$

— for two-dimensional, four-node linear elements, with consistent capacity matrices:

$$[\lambda_1, \dots, \lambda_4] = \left[0, -\frac{12\alpha}{\Delta x^2}, -\frac{12\alpha}{\Delta y^2}, -\left(\frac{12\alpha}{\Delta x^2} + \frac{12\alpha}{\Delta y^2}\right) \right] \quad (\text{A4})$$

— for two-dimensional, four-node linear elements, with lumped capacity matrices:

$$[\lambda_1, \dots, \lambda_4] = \left[0, -\frac{4\alpha}{\Delta x^2}, -\frac{4\alpha}{\Delta y^2}, -\left(\frac{4\alpha}{\Delta x^2} + \frac{4\alpha}{\Delta y^2}\right) \right] \quad (\text{A5})$$

— for two-dimensional, eight-node parabolic elements, with consistent capacity matrices:

$$[\lambda_1, \dots, \lambda_8] = \left[0, -\frac{3\alpha}{\Delta x^2}, -\frac{3\alpha}{\Delta y^2}, -\left(\frac{3\alpha}{\Delta x^2} + \frac{3\alpha}{\Delta y^2}\right), \right. \\ \left. -\frac{15\alpha}{\Delta x^2}, -\frac{15\alpha}{\Delta y^2}, -\left(\frac{3\alpha}{\Delta x^2} + \frac{15\alpha}{\Delta y^2}\right), -\left(\frac{15\alpha}{\Delta x^2} + \frac{3\alpha}{\Delta y^2}\right) \right] \quad (\text{A6})$$

— for three-dimensional, eight-node linear elements, with consistent capacity matrices:

$$[\lambda_1, \dots, \lambda_8] = \left[0, -\frac{12\alpha}{\Delta x^2}, -\frac{12\alpha}{\Delta y^2}, -\frac{12\alpha}{\Delta z^2}, -\left(\frac{12\alpha}{\Delta x^2} + \frac{12\alpha}{\Delta y^2}\right), \right. \\ \left. -\left(\frac{12\alpha}{\Delta x^2} + \frac{12\alpha}{\Delta z^2}\right), -\left(\frac{12\alpha}{\Delta y^2} + \frac{12\alpha}{\Delta z^2}\right), -\left(\frac{12\alpha}{\Delta x^2} + \frac{12\alpha}{\Delta y^2} + \frac{12\alpha}{\Delta z^2}\right) \right] \quad (\text{A7})$$

— for three-dimensional, eight-node linear elements, with lumped capacity matrices:

$$[\lambda_1, \dots, \lambda_8] = \left[0, -\frac{3\alpha}{\Delta x^2}, -\frac{3\alpha}{\Delta y^2}, -\frac{3\alpha}{\Delta z^2}, -\left(\frac{3\alpha}{\Delta x^2} + \frac{3\alpha}{\Delta y^2}\right), \right. \\ \left. -\left(\frac{3\alpha}{\Delta x^2} + \frac{3\alpha}{\Delta z^2}\right), -\left(\frac{3\alpha}{\Delta y^2} + \frac{3\alpha}{\Delta z^2}\right), -\left(\frac{3\alpha}{\Delta x^2} + \frac{3\alpha}{\Delta y^2} + \frac{3\alpha}{\Delta z^2}\right) \right] \quad (\text{A8})$$

— for three-node, equilateral triangular elements, with consistent capacity matrices:

$$[\lambda_1, \dots, \lambda_3] = \left[0, -\frac{24\alpha}{\Delta L^2}, -\frac{24\alpha}{\Delta L^2} \right] \quad (\text{A9})$$

— for three-node, equilateral triangular elements, with lumped capacity matrices:

$$[\lambda_1, \dots, \lambda_3] = \left[0, -\frac{6\alpha}{\Delta L^2}, -\frac{6\alpha}{\Delta L^2} \right] \quad (\text{A10})$$

— for three-node, right triangular elements, with consistent capacity matrices:

$$[\lambda_1, \dots, \lambda_3] = \left[0, -\frac{12\Delta x^2 + 12\Delta y^2 - 12\sqrt{\Delta x^4 - \Delta x^2\Delta y^2 + \Delta y^4}}{\Delta x^2\Delta y^2}, \right. \\ \left. -\frac{12\Delta x^2 + 12\Delta y^2 + 12\sqrt{\Delta x^4 - \Delta x^2\Delta y^2 + \Delta y^4}}{\Delta x^2\Delta y^2} \right] \quad (\text{A11})$$

— for three-node, right triangular elements, with lumped capacity matrices:

$$[\lambda_1, \dots, \lambda_3] = \left[0, -\frac{3\Delta x^2 + 3\Delta y^2 - 3\sqrt{\Delta x^4 - \Delta x^2\Delta y^2 + \Delta y^4}}{\Delta x^2\Delta y^2}, \right. \\ \left. -\frac{3\Delta x^2 + 3\Delta y^2 + 3\sqrt{\Delta x^4 - \Delta x^2\Delta y^2 + \Delta y^4}}{\Delta x^2\Delta y^2} \right] \quad (\text{A12})$$

— for four-node, equilateral tetrahedral elements, with consistent capacity matrices:

$$[\lambda_1, \dots, \lambda_4] = \left[0, -\frac{40\alpha}{\Delta L^2}, -\frac{40\alpha}{\Delta L^2}, -\frac{40\alpha}{\Delta L^2} \right] \quad (\text{A13})$$

— for four-node, equilateral tetrahedral elements, with lumped capacity matrices:

$$[\lambda_1, \dots, \lambda_4] = \left[0, -\frac{8\alpha}{\Delta L^2}, -\frac{8\alpha}{\Delta L^2}, -\frac{8\alpha}{\Delta L^2} \right] \quad (\text{A14})$$

— for four-node, right tetrahedral elements, with equal sides and consistent capacity matrices:

$$[\lambda_1, \dots, \lambda_4] = \left[0, -\frac{20\alpha}{\Delta L^2}, -\frac{20\alpha}{\Delta L^2}, -\frac{80\alpha}{\Delta L^2} \right] \quad (\text{A15})$$

— for four-node, right isosceles tetrahedral elements, with lumped capacity matrices:

$$[\lambda_1, \dots, \lambda_4] = \left[0, -\frac{4\alpha}{\Delta L^2}, -\frac{4\alpha}{\Delta L^2}, -\frac{16\alpha}{\Delta L^2} \right] \quad (\text{A16})$$

APPENDIX B

By going through the steps outlined in the text, we have computed the eigenvectors for most of the elements represented in *Figure 1*. To deal with integer numbers, the entries in the eigenvectors have been scaled, but no attempt has been made to arrive at sets of orthonormal vectors. From the numerical results it appears that no distinction can be made between consistent and lumped capacity matrices⁷ and, consequently, the results obtained can be listed as follows:

— for one-dimensional, two node linear elements:

$$\begin{aligned} \phi_1 &= [1, 1]^T \\ \phi_2 &= [-1, 1]^T \end{aligned} \quad (\text{B1})$$

— for one-dimensional, three-node parabolic elements:

$$\begin{aligned} \phi_1 &= [1, 1, 1]^T \\ \phi_2 &= [-1, 0, 1]^T \\ \phi_3 &= [-2, 1, -2]^T \end{aligned} \quad (\text{B2})$$

— for two-dimensional, four-node linear elements:

$$\begin{aligned} \phi_1 &= [1, 1, 1, 1]^T \\ \phi_2 &= [-1, 1, 1, -1]^T \\ \phi_3 &= [-1, -1, 1, 1]^T \\ \phi_4 &= [-1, 1, -1, 1]^T \end{aligned} \quad (\text{B3})$$

— for two-dimensional, eight-node parabolic elements:

$$\begin{aligned} \phi_1 &= [1, 1, 1, 1, 1, 1, 1, 1]^T \\ \phi_2 &= [-1, 0, 1, 1, 1, 0, -1, -1]^T \\ \phi_3 &= [-1, -1, -1, 0, 1, 1, 1, 0]^T \\ \phi_4 &= [-1, 0, 1, 0, -1, 0, 1, 0]^T \\ \phi_5 &= [-2, 1, -2, -2, -2, 1, -2, -2]^T \\ \phi_6 &= [-2, 1, -2, 0, 2, -1, 2, 0]^T \\ \phi_7 &= [-2, 0, 2, -1, 2, 0, -2, 1]^T \\ \phi_8 &= [-2, 1, -2, 0, 2, -1, 2, 0]^T \end{aligned} \quad (\text{B4})$$

— for three-dimensional, eight-node linear elements:

$$\begin{aligned}
 \phi_1 &= [1, 1, 1, 1, 1, 1, 1, 1]^T \\
 \phi_2 &= [1, -1, -1, 1, 1, -1, -1, 1]^T \\
 \phi_3 &= [1, 1, -1, -1, 1, 1, -1, -1]^T \\
 \phi_4 &= [1, 1, 1, 1, -1, -1, -1, -1]^T \\
 \phi_5 &= [1, -1, 1, -1, 1, -1, 1, -1]^T \\
 \phi_6 &= [1, -1, -1, 1, -1, 1, 1, -1]^T \\
 \phi_7 &= [1, 1, -1, -1, -1, -1, 1, 1]^T \\
 \phi_8 &= [1, -1, 1, -1, -1, 1, -1, 1]^T
 \end{aligned}
 \tag{B5}$$

— for three-node, equilateral triangular elements:

$$\begin{aligned}
 \phi_1 &= [1, 1, 1]^T \\
 \phi_2 &= [-1, 0, 1]^T \\
 \phi_3 &= [-1, 1, 0]^T
 \end{aligned}
 \tag{B6}$$

— for three-node, right triangular elements:

$$\begin{aligned}
 \phi_1 &= [1, 1, 1]^T \\
 \phi_2 &= \left[1, \frac{-\Delta x^2 - \sqrt{\Delta x^4 - \Delta x^2 \Delta y^2 + \Delta y^4}}{\Delta x^2 - \Delta y^2}, \frac{+\Delta y^2 + \sqrt{\Delta x^4 - \Delta x^2 \Delta y^2 + \Delta y^4}}{\Delta x^2 - \Delta y^2} \right]^T \\
 \phi_3 &= \left[1, \frac{-\Delta x^2 + \sqrt{\Delta x^4 - \Delta x^2 \Delta y^2 + \Delta y^4}}{\Delta x^2 - \Delta y^2}, \frac{+\Delta y^2 - \sqrt{\Delta x^4 - \Delta x^2 \Delta y^2 + \Delta y^4}}{\Delta x^2 - \Delta y^2} \right]^T
 \end{aligned}
 \tag{B7}$$

— for four-node, equilateral tetrahedral elements:

$$\begin{aligned}
 \phi_1 &= [1, 1, 1, 1]^T \\
 \phi_2 &= [-1, 0, 0, 1]^T \\
 \phi_3 &= [-1, 0, 1, 0]^T \\
 \phi_4 &= [-1, 1, 0, 0]^T
 \end{aligned}
 \tag{B8}$$

— for four-node, right tetrahedral elements, with equal sides:

$$\begin{aligned}
 \phi_1 &= [1, 1, 1, 1]^T \\
 \phi_2 &= [0, -1, 0, 1]^T \\
 \phi_3 &= [0, -1, 1, 0]^T \\
 \phi_4 &= [-3, 1, 1, 1]^T
 \end{aligned}
 \tag{B9}$$